OPEN ACCESS

International Journal of Innovations in Science & Technology

Preparation of CuSe Thin Films by Chemical Vapor Deposition via Water Splitting for Hydrogen Generation

Joun Ali Faraz, Sana Tariq, M. Bilal, Tanvir Hussain*

The University of Management and Technology, Lahore, Punjab 54770

***Correspondence**: tanvir.hussain@umt.edu.pk*, joun.faraz@umt.edu.pk, muhammad.bilal@umt.edu.pk,

Citation | Faraz. J. A, Tariq. S, Bilal. M, Hussain. T, “Preparation of CuSe Thin Films by Chemical Vapor Deposition via Water Splitting for Hydrogen Generation”, IJIST, Vol. 07 Issue. 03 pp 1353-1364, July 2025

Received| June 05, 2025 **Revised|** June 28, 2025 **Accepted|** July 02, 2025 **Published|** July 09, 2025.

In recent years, significant research has been done on semiconductor heterostructures to produce hydrogen by water splitting. The absorption of visible light and photoelectrochemical properties of CuO thin film are enhanced by the selenization. The selenization of CuO thin film is done by chemical vapor deposition (CVD) at various temperatures. The structural properties of the prepared samples were characterized by XRD, and the morphological properties of the prepared film were characterized by scanning electron microscopy. Optical properties reveal that the bandgap was decreased by increasing the selenization temperature. The solar light to hydrogen conversion efficiency of the CuSe-500°C, CuSe-600°C, and CuSe-650°C films were estimated by using three-electrode cells. It was noticed that CuSe-650°C showed much better STH% compared to pristine CuO thin film.

Keywords: Semiconductor Heterostructures, Hydrogen Production, Morphological Analysis, Three-Electrode Cell, Cuse-500°C, Cuse-600°C, Cuse-650°C

Introduction:

The rapid pace of economic development, coupled with a growing global population, has significantly escalated energy demand, presenting a serious threat to human sustainability. In addition, there has been a significant rise in greenhouse gases in the atmosphere as a result of the widespread use of fossil fuels and industrial waste [1]. The use of renewable energy sources like wind, solar, and tidal energy has enormous promise for future populations. The quantity of solar energy on Earth and its lack of danger make it the most attractive of them [2].

Hydrogen is a desirable, environmentally benign fuel that may be used for a number of purposes, including heating, driving vehicles, and material recycling. Its high energy density and compatibility with both internal combustion engines and fuel cells make it a promising alternative to fossil fuels, positioning it as a key component in the future of emission-free transportation [3][4][5]. In addition, a number of water-splitting technologies have been discovered, including electrochemical, thermochemical, photocatalytic, photoelectrochemical (PEC), and biohydrogen production. One of them, PEC water splitting, converts solar energy into hydrogen, which may subsequently be utilized for a variety of other energy-related applications [6]. Photoelectrochemical (PEC) water splitting is considered one of the most promising technologies for hydrogen production due to its inherent safety, non-toxicity, and the clean nature of its reaction, which produces only pure hydrogen and oxygen without any harmful byproducts [7].

The current global energy consumption stands at approximately 18.5 terawatts (TW), and this demand is expected to rise further in the future as a result of ongoing industrialization and population growth. In 2050, the demand is predicted to increase to as much as 50 TW [8]. These gases into the atmosphere, raising concentrations of greenhouse gases, which warms the Earth's climate and has an influence on environmental change (carbon dioxide, methane, nitrous oxide). It is clear that carbon dioxide has just recently entered the atmosphere, and human activity is causing it to increase, which has an impact on the environment. The most effective way to reduce carbon dioxide emissions and reduce the consumption of fossil fuels. The photocatalytic activity of any metal oxide can be significantly improved through nanostructuring and by enhancing its ability to absorb solar light [9]. Nanostructures offer a higher surface area, making them a promising approach to boosting photocatalytic efficiency [10][11].

According to reports, semiconductors with hierarchical hollow shells, mesoporous thin films, and nanocrystalline thin films have superior photocatalytic activity compared to bulk semiconductor material [11]. To assess the materials' capacity for photocatalysis, nanoporous and nano flask CuSe and assessed for the photocurrent density. The nano-structuring of CuSe was found to significantly enhance photocurrent density, highlighting the improved performance of the nanoporous and nanoflask morphologies.

Photoelectrochemical water splitting is the most important process to produce hydrogen from water via solar energy. A Photoelectrochemical cell is based on the translation of light energy into electricity in the form of hydrogen within a cell involving two electrodes [12][13]. In this setup, one electrode functions as the cathode while the other serves as the anode. Among these, one must act as the photoelectrode, meaning it responds when exposed to direct sunlight. In this study, a photoanode is used, which is composed of a semiconductor material capable of absorbing light and initiating the photoelectrochemical reaction upon illumination. [13].

The solar-to-hydrogen (STH) efficiency of photocatalytic water splitting has remained low, primarily due to limited light absorption and sluggish oxidation reactions. To enhance STH efficiency, this study aims to utilize a clean water-splitting catalyst that effectively harnesses sunlight [14]. The type of solar cell or photocatalyst employed, the wavelength and intensity of the sun's radiation, and the water-splitting processes are some of the variables that affect STH efficiency. Higher efficiency in the system results in greater conversion of solar energy into hydrogen [14][15][16].

Literature Review:

Nanostructured CuO thin films are fabricated using thermal evaporation followed by annealing. Structural, optical, and morphological changes induced by the annealing process are analyzed using X-ray diffraction (XRD), UV–Visible absorption spectroscopy, atomic force microscopy (AFM), and field emission scanning electron microscopy (FESEM). These changes are further correlated with the films' photocatalytic performance. Thermal annealing results in notable changes in the morphological, optical, structural, and photocatalytic activity of nanostructured CuO thin films. CuO nanoparticles are produced using thermal annealing, and when the annealing temperature is raised to 600ºC, the average size of the CuO nanoparticles rises from 23nm to 293nm [17].

The formation of an abundance of materials with varied and adaptable electrical, optical, and chemical characteristics has led to an increase in research interest in two-dimensional (2D) materials. Moreover, heterostructures based on 2D materials that combine numerous distinct 2D materials offer special platforms for the creation of an almost unlimited variety of materials, as well as the demonstration of novel physical phenomena, features, and applications [18]. To meet these high standards, techniques for the scalable preparation of high-quality, inexpensive 2D heterostructures and 2D materials are needed. Despite some initial ongoing difficulties, chemical vapor deposition (CVD), a potent technique that may satisfy the aforementioned criteria, has been widely employed to build 2D materials and associated heterostructures in recent years [19]. In this study, the current developments in the controlled growth of single-crystal 2D materials, with a focus on semiconducting transition metal dichalcogenides, are assessed in an assessment of the difficulties in the CVD formation of 2D materials [20].

The author reported that cuprous oxide is one of the possible active layers for solar systems based on semiconductor oxides (Cu_2O). This oxide semiconductor exhibits a variety of desirable properties that are advantageous for the construction of solar cells, including affordability, minority mobility of carriers, and diffusion length are also large, as is the absorption coefficient and direct energy gap. This article presents the findings from optical and structural investigations of Cu_2O thin films formed by thermal vacuum evaporation of CuO powder. The structural and optical properties of Cu_2O films are studied as a function of deposition velocity [21].

The author mentioned the structural, optical, and electrical characteristics of copper selenide thin films (0.05-0.25μm) made in chemical baths with sodium selenosulfate or N, N-dimethylselenourea as the selenide ion source. The films produced by baths containing sodium selenosulfate appear to have a cubic structure similar to that of berzelianite, $Cu_{2-x}Se$ with x=0.15. The films are partially converted to Cu_2Se by annealing them at 400°C in nitrogen. The XRD patterns of the films made from baths containing dimethylselenourea correspond to those of klockmannite, CuSe. The XRD patterns of films prepared from baths containing dimethylselenourea correspond to the klockmannite phase, CuSe. Upon annealing in nitrogen at 400 °C, selenium is lost, resulting in the formation of a copper-rich composition such as $Cu_{2-x}Se$ [22].

Objectives:

- CuSe thin films are deposited via chemical vapor deposition (CVD) and water splitting.
- To determine how selenization temperature (500°C, 600°C, and 650°C) affects the structural, morphological, and optical aspects of CuSe thin films.

- To assess the photoelectrochemical (PEC) performance of CuSe films in terms of photocurrent density and solar-to-hydrogen conversion efficiency.

Novelty:

To synthesize CuSe thin films, this study utilizes a unique technique that combines water splitting with the selenization of CuO films by CVD. Unlike most previous studies, which focus on either CuO or CuSe, this work systematically investigates how changing the selenization temperature affects film characteristics and increases hydrogen production efficiency. The determination of the ideal processing temperature (650°C) for best PEC performance provides a realistic approach to improving solar hydrogen generation.

Research Methodology:

Growth of the Cu Layer by Thermal Evaporation:

CuO thin films were initially deposited using the thermal evaporation method. Following this, CuSe films were developed through a chemical vapor deposition (CVD) process. Before film deposition, the resistivity of the ITO substrates was measured using a multimeter to ensure suitability. The glass substrates were then mounted onto the substrate holder positioned at the top of the vacuum chamber lid in the thermal evaporator. Subsequently, high-purity copper oxide powder (99.98%) obtained from Sigma-Aldrich was loaded into a tungsten boat positioned at the bottom of the vacuum chamber. Once a vacuum level of 10^{-5} mbar was achieved in the chamber, the power supply of the transformer was switched on, and the current was applied. As the tungsten boat was heated, the pure copper oxide powder inside began to evaporate and subsequently deposited onto the surface of the substrate.

Growth of the CuSe layer by Chemical Vapour Deposition:

The thin layer of CuSe was prepared in a single-zone horizontal quartz tube furnace. An alumina boat was taken and filled with pure selenium powder obtained from Sigma-Aldrich. The CuO thin film was used as a substrate, as a layer of selenium was to be deposited on it to form CuSe. A rotary van pump was connected to the tube furnace of the CVD to create a vacuum up to 10^{-2} mbar. As selenium powder starts to evaporate, we supply the argon gas from the gas cylinder for 20 minutes into the tube furnace as a carrier gas, and the evaporated selenium is deposited on the substrates. We achieve a very fine thin film of CuSe. The deposited films were annealed at varying temperatures (500°C, 600°C, and 650°C) in a vacuum tube furnace to enhance crystallinity and optimize band alignment.

The structural properties of the materials were determined by XRD. The samples were analyzed using a Bruker D2 Phaser X-ray diffractometer to study their structural properties. XRD pattern provides information about the phase and purity of the sample. The crystallite size of the prepared samples was also estimated using the Debye–Scherrer formula. The surface morphology of CuSe films was investigated using an SEM with a 5 kV accelerating voltage and an 8 mm working distance. The secondary electron detection technique was used with a 10 µs stay period per pixel. SEM is based on the interaction of an electron beam with a sample's atoms at different depths and reveals the information in the signal form (backscattered electrons, secondary electrons, x-rays, etc) that gives information about the sample's surface composition and topography. A spectrophotometer is an optical instrument used to measure the absorbance and transmittance of a sample at different wavelengths when a beam of monochromatic light passes through it. In this work, a Cary 60 UV-Vis spectrophotometer was used, operating in the wavelength range of 200 to 800 nm. A clean glass substrate was used for baseline correction, and spectra were recorded at 1 nm resolution. A spectrophotometer is based on Beer and Lambert's Law, which states that the amount of light absorbed by a sample is directly proportional to the concentration and the path length (thickness) of the sample. The photoelectrochemical cell consists of three main parts. The working electrode is made of a semiconductor (photoanode), and the reference electrode is made of platinum and water, which is an electrolyte (KCl, Na_2SO_4). The photoelectrochemical (PEC) cell consisted of an electrolyte-filled chamber with two electrodes immersed in it. The CuSe and pure CuO thin films behave like a working photoanode with a 0.5M solution of KOH serving as the electrolyte. The scan rate was set at 100mV/s with a starting voltage range of 1.0V to +1.0V to obtain the J-V graph using Linear Sweep Voltammetry under dark and light conditions. The following formula is used to measure photocurrent density.

$$\text{Photocurrent density} = \text{Jphoto} = \text{Jlight} - \text{Jdark} \quad (1)$$

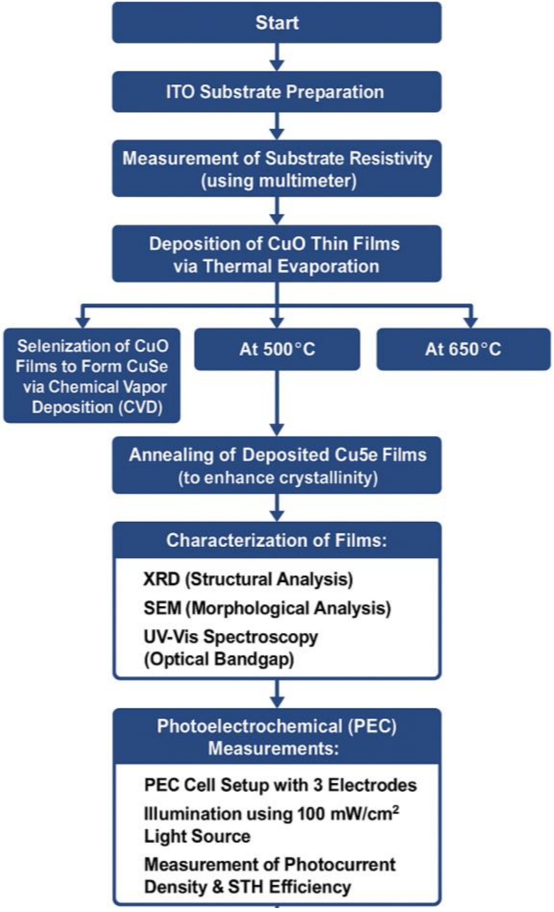

Figure 1. Flow Diagram of Methodology

Results and Discussion:

Structural Analysis:

Figure 2 shows the XRD pattern of CuSe annealed at 500 °C. Figure 2.1(a) displays diffraction peaks located at 2θ values of 24.15°, 27.07°, 31.13°, 46.48°, and 55.70°, corresponding to the (101), (102), (006), (110), and (116) crystal planes, respectively. All diffraction peaks were well matched to the (JCPDS card no. 34-0171). The XRD pattern of the CuSe-600°C Figure 2(b) shows the diffraction peaks located at 2θ= 23.92°, 27.18°, 30.90°, 46.73°, and 55.58° which correspond to the (101), (102), (006), (110), and (116) crystal planes, respectively. All diffraction peaks are well matched to the (JCPDS card no. 34-0171) [23]. The XRD pattern of the CuSe-650°C Figure 2(c) shows the diffraction peaks located at 2θ= 24.03°, 31.02°, 46.49°, and 55.70° which correspond to the (101), (006), (110), and (116) crystal planes, respectively. The CuSe thin films developed at 500 °C, 600 °C, and 650 °C exhibited a hexagonal crystal structure. The crystallinity of the films was improved with an increase in film thickness.

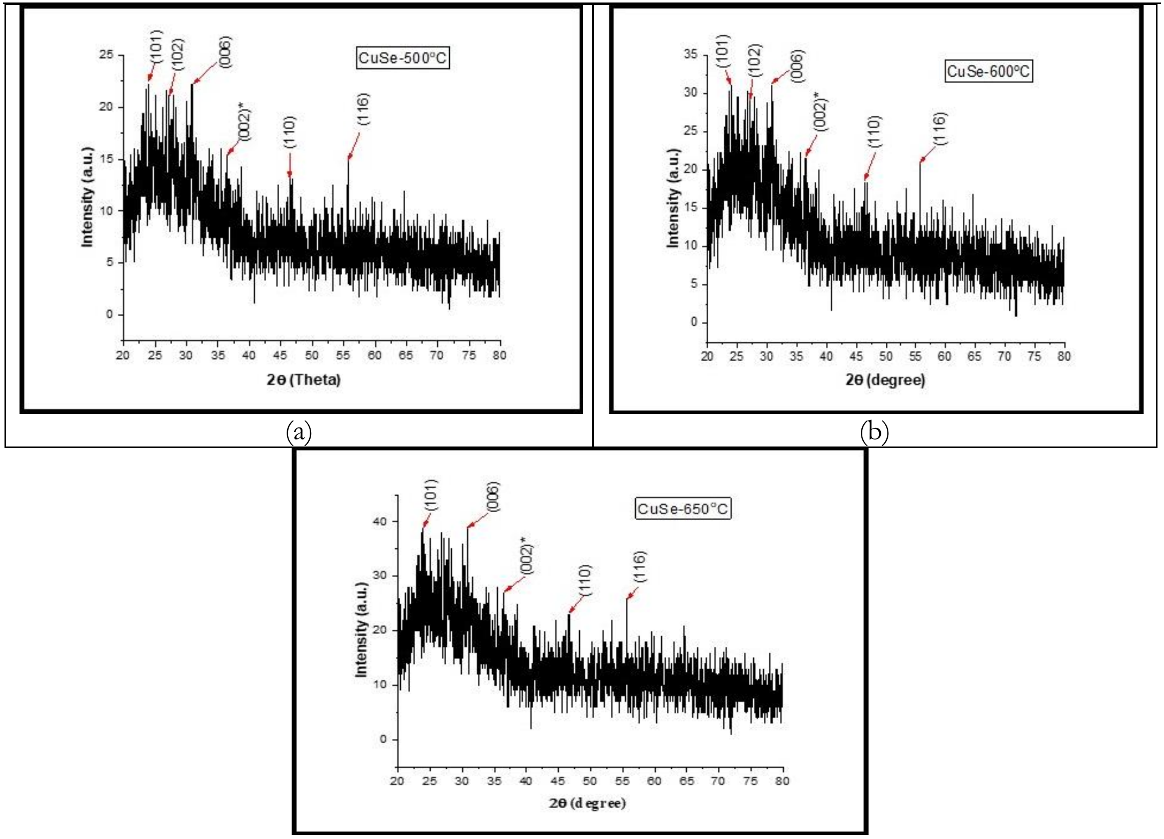

(a) (b)

(c)

Figure 2. Represents the XRD patterns of CuSe-500 °C (a), CuSe -600 °C (b), and CuSe -650 °C (c) thin films

Morphological Properties:

The morphological properties of the CuSe thin films prepared at 500°C, 600°C, and 650°C are measured by scanning electron microscopy (SEM). The surface morphology of the CuSe film prepared at 500°C examined by SEM is shown in Figure 3 (a) and (b) with the resolution of 1µm and 200 nm, respectively. The images clearly show that the film has a granular structure, and agglomeration of particles is also observed. SEM image depicts that the surface almost looks smooth and no creaks, voids, or empty spaces are present. It shows that the particle size lies in the range of 100 nm to 200 nm. The microstructure of the films was significantly affected by the annealing temperature.

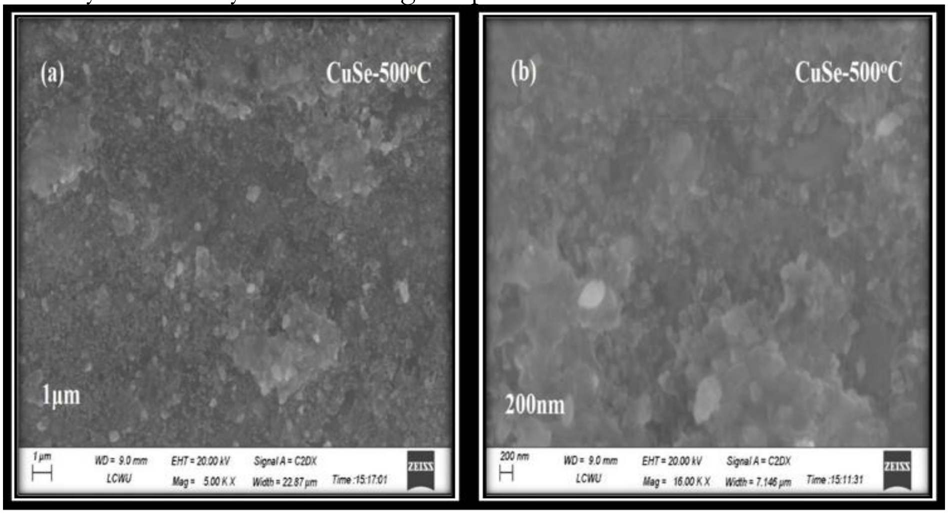

Figure 3. SEM images for CuSe-500°C thin film at 1µm and 200nm resolutions

The surface morphology of the CuSe film at 600°C examined by SEM is shown in Figure 4 (a) and (b) with the resolution of 1µm and 200nm, respectively. SEM images revealed that the film is smooth, and at some point, we can see the agglomeration of particles on the surface of the CuSe thin film. Therefore, the surface of the CuSe film appears smoother compared to the CuSe-500 °C sample, due to selenization at the higher temperature of 600 °C. No cracks, voids, or empty spaces are observed on the film's surface.

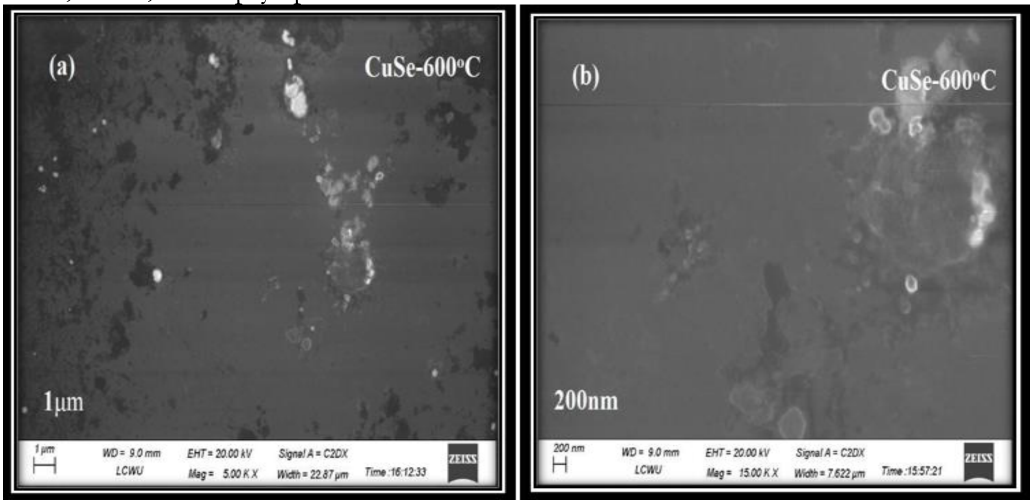

Figure 4. SEM images for CuSe-600°C thin film at 1µm and 200nm resolutions

The surface morphology of the CuSe film at 650°C examined by SEM is shown in Figure 5 (a) and (b) with the resolution of 1µm and 200nm, respectively. SEM images revealed that the film is smooth, but in some regions, empty spaces are observed. In the empty spaces, numerous particles of varying sizes can be observed, ranging from 100 nm to 300 nm. The formation of empty spaces is attributed to high-temperature annealing.

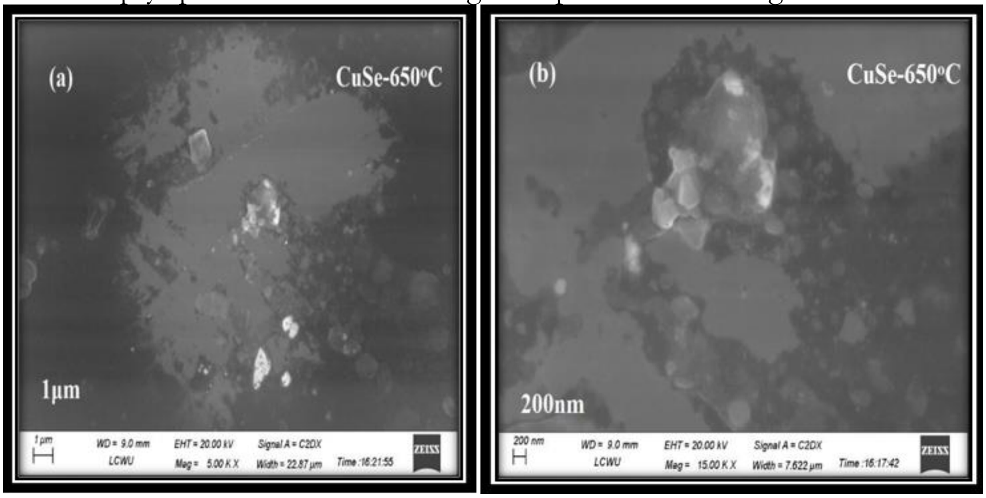

Figure 5. SEM images for CuSe-650°C thin film at 1µm and 200nm resolutions

Optical Properties:

Figure 6 shows the transmittance spectra of a glass substrate, CuO, and CuSe-500°C, CuSe-600°C, and CuSe-650°C thin films. It was observed that the transmittance of CuSe decreased as the temperature increased from 500 °C to 600 °C, but then increased again when the temperature was raised from 600 °C to 650 °C. The decrease in transmittance might be due to the diffusion of Se atoms into the CuO thin film, which could introduce structural defects. With a further increase in temperature, Se may react with Cu and facilitate the removal of oxygen from the film. The decrease in the number of structural defects resulted in less scattering, and thus increased the transmittance of CuSe.

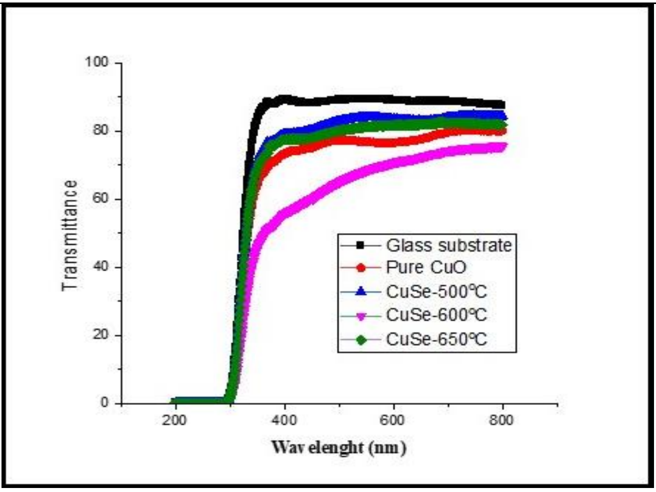

Figure 6. Transmittance spectra of all samples

Determination of Bandgap:

Figure 7 (a) shows the Tauc plot of CuO thin film. The linear part of the curve was fitted to estimate the optical bandgap of pure CuO. The calculated value of the optical bandgap for pure CuO is 2.50eV, which is greater than the bandgap of bulk CuO 1.30eV. Figure 7(b) shows the optical bandgap of the CuSe thin film annealed at a temperature of 500°C was based on the transmittance measurement. The linear part of the curve was fitted to measure the optical bandgap. So, the value of the bandgap of CuSe-500°C is 2.40eV. Figure 7 (c) shows the bandgap of CuSe annealed at a temperature of 600°C. For the CuSe thin film, the value of the band gap was found by the linear portion of the

Tauc plot on the x-axis. The calculated value of the band gaps of CuSe-600°C thin film is 2.13eV. Figure 7 (d) shows the optical bandgap of CuSe thin film annealed at a temperature of 650°C. By plotting the graph of $(\alpha h\nu)^2$ versus photon energy, a strong linear relationship was observed, indicating the bandgap value of the CuSe thin film annealed at 650 °C. The value of the bandgap of CuSe-650°C is 2.10eV. The energy bandgap of the CuSe thin film decreases with the increase of temperatures from 500°C-650°C due to the increase in crystallinity and decrease in defects. The decrease in band gap with an increase in temperature is also attributed to the increase in grain size of the crystallite with an increase in the thickness of the film.

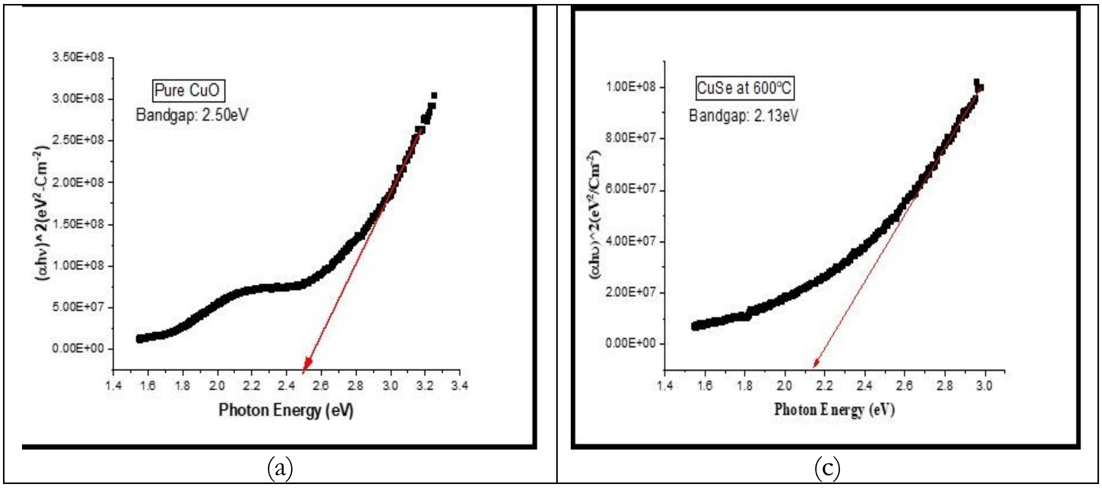

(a) (c)

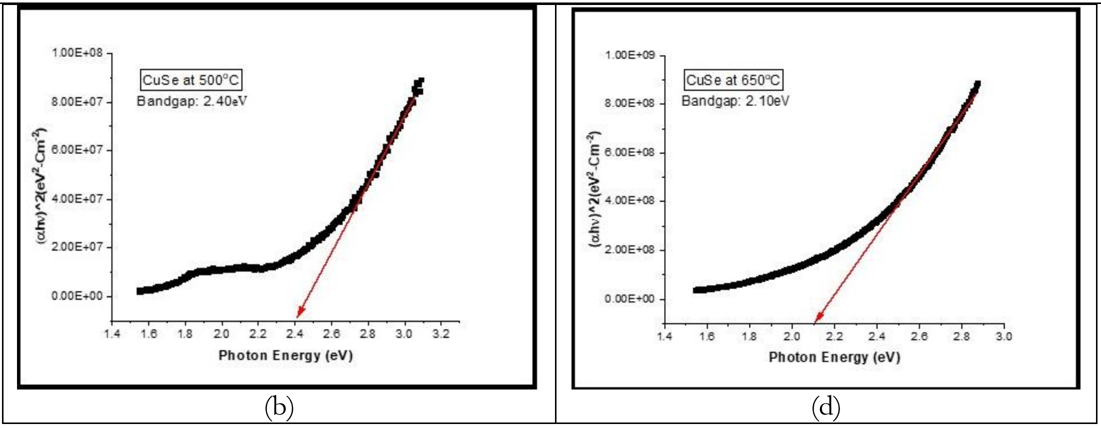

(b) (d)

Figure 7. Tauc plot for as-deposited CuO, Figure(a), CuSe-500 °C, Figure(b), CuSe-600°C Figure(c), CuSe-650°C Figure(d).

Photoelectrochemical Water Splitting:

Pure CuO has a relative photocurrent density of 0.3247 mA/cm^2. The relative photocurrent density of the CuSe heterostructure thin film after annealing at 500 is 3.633 mA/cm^{2,} while at 600°C it is 1.222 mA/cm^2. However, at 650 °C, the photocurrent density significantly increases to 8.6 mA/cm^2, which is the highest among all the measured values. Subsequently, further increase in temperature, the photocurrent density increased. The initial decrease in photocurrent density is attributed to the presence of Se atoms on the surface, which reduces the generation of electron-hole pairs. However, with a further increase in temperature, electron-hole recombination decreases and a more favorable energy gradient for charge transfer is established, resulting in enhanced photocurrent. The photocurrent density of pure CuO is low due to its relatively high bandgap, which limits the absorption of solar light.

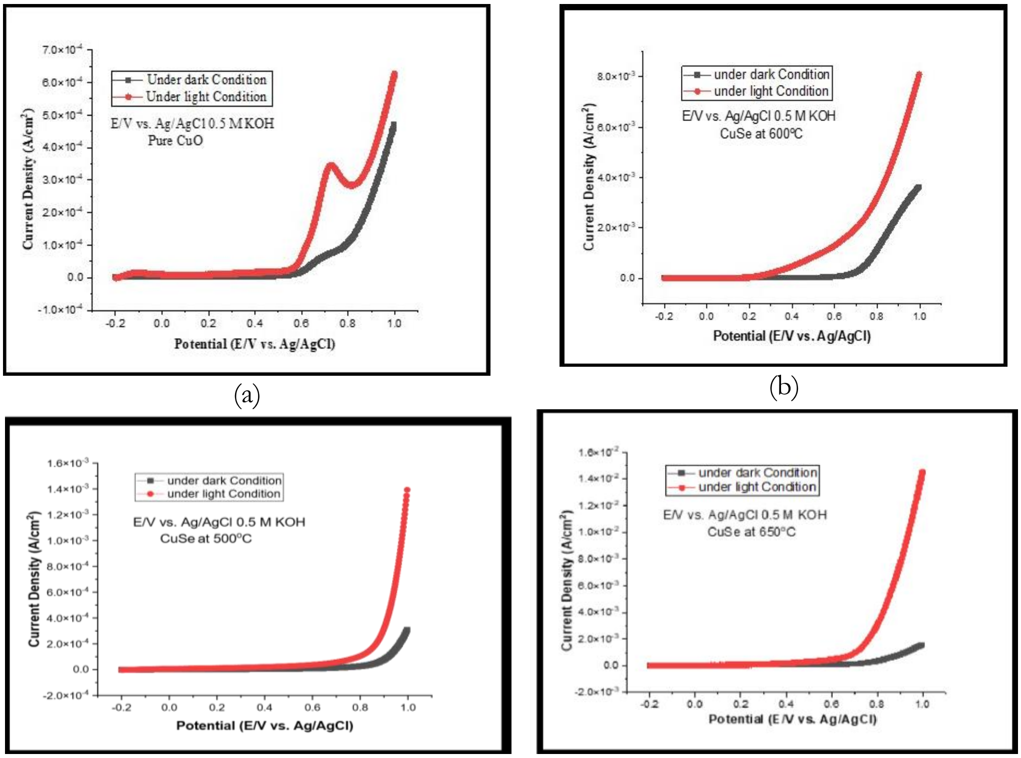

(a) (b)

(c) (d)

Figure 8. LSV Graphs of Pure CuO Figure(a), Pure CuSe-500°C Figure(b), CuSe-600°C Figure(c), CuO650 °C Figure(d) thin films under dark and light conditions.

Solar to Hydrogen Conversion Efficiency:

The performance of the working electrode was estimated by measuring the solar light to hydrogen conversion efficiency. The following formula of STH% is

$$\mathbf{STH\%} = \frac{(1.23-\text{Vbias})\times j}{P}\times\mathbf{100}\% \quad (2)$$

Where P is the intensity of the solar spectrum, V_{bias} is the applied voltage, and j is the photocurrent density.

Samples	STH%
CuO	0.3502%
CuSe-500^{O}C	0.2507%
CuSe-600^{O}C	1.012%
CuSe-650^{O}C	2.967%

All the calculated values of Solar to hydrogen conversion efficiency in percentage are plotted in Figure 9 below. It was observed that the solar-to-hydrogen efficiency (STH%) increased with the rising selenization temperature of CuO. The highest STH% was recorded for the CuSe thin film annealed at 650 °C.

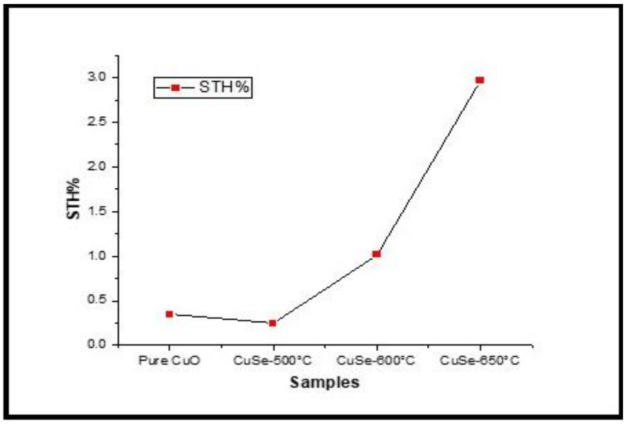

Figure 9. STH% of all the samples

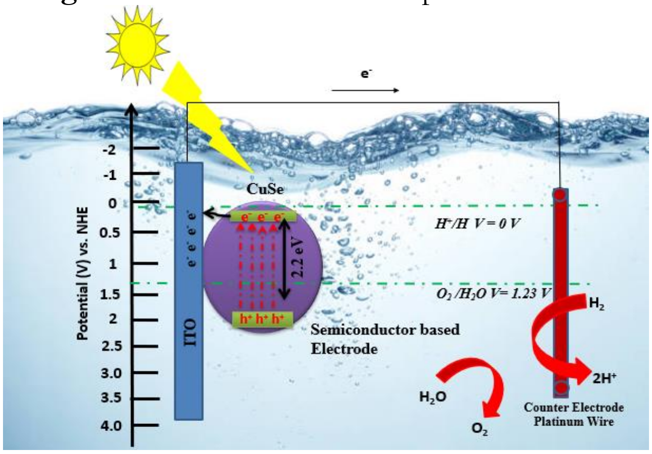

Figure 10. Plausible reaction mechanism of CuSe thin film-based photocatalyst for H_2 generation under solar light irradiation.

Conclusions:

CuSe thin films were successfully produced by selenizing CuO using CVD at different temperatures. Polycrystallinity has been confirmed by structural investigation, with some residual CuO present at lower temperatures. SEM analysis revealed that surface morphology improved as temperatures increased. Optical properties determined that the bandgap decreased with increasing selenization temperature, indicating increased crystallinity. Particularly, CuSe-650°C had the highest photocurrent density and solar-to-hydrogen (STH) efficiency (2.967%), indicating its promise as a photoelectrode material for solar hydrogen generation. Overall, increasing the selenization temperature increases the optoelectronic and photoelectrochemical properties of CuSe thin films.

References:

[1] P. L. S. Luqman Jeffry, Mei Yin Ong, Saifuddin Nomanbhay, M. Mofijur, Muhammad Mubashir, “Greenhouse gases utilization: A review,” *Fuel*, vol. 301, p. 121017, 2021, doi: https://doi.org/10.1016/j.fuel.2021.121017.

[2] M. M. H. Abidur Rahman, Omar Farrok, “Environmental impact of renewable energy source based electrical power plants: Solar, wind, hydroelectric, biomass, geothermal, tidal, ocean, and osmotic,” *Renew. Sustain. Energy Rev.*, vol. 161, p. 112279, 2022, [Online]. Available: https://www.sciencedirect.com/science/article/abs/pii/S136403212200199X?via%3Dihub

[3] D.-V. N. V. Fazil Qureshi, Mohammad Yusuf, Hussameldin Ibrahim, Hesam Kamyab, Shreeshivadasan Chelliapan, Cham Q. Pham, “Contemporary avenues of the Hydrogen industry: Opportunities and challenges in the eco-friendly approach,” *Environ. Res.*, vol. 229, p. 115963, 2023, [Online]. Available: https://www.sciencedirect.com/science/article/abs/pii/S0013935123007557?via%3Dihub

[4] H. Z. A Onorati, R Payri, “The role of hydrogen for future internal combustion engines,” *Sage Journals*, vol. 23, no. 4, 2022, doi: https://doi.org/10.1177/14680874221081947.

[5] S. P. Pawan Kumar Pathak, Anil Kumar Yadav, “Transition toward emission-free energy systems by 2050: Potential role of hydrogen,” *Int. J. Hydrogen Energy*, vol. 48, no. 26, pp. 9921–9927, 2023, [Online]. Available: https://www.sciencedirect.com/science/article/abs/pii/S0360319922057755?via%3Dihub

[6] S. Imran and M. Hussain, “Emerging trends in water splitting innovations for solar hydrogen production: Analysis, comparison, and economical insights,” *Int. J. Hydrogen Energy*, vol. 77, pp. 975–996, 2024, [Online]. Available: https://www.sciencedirect.com/science/article/abs/pii/S036031992402490X?via%3Dihub

[7] F. P. B. Inês Rolo, Vítor A. F. Costa, “Hydrogen-Based Energy Systems: Current Technology Development Status, Opportunities and Challenges,” *Energies*, vol. 17, no. 1, p. 180, 2024, doi: https://doi.org/10.3390/en17010180.

[8] R. V. Jerry L. Holechek, Hatim M. E. Geli, Mohammed N. Sawalhah, “A Global Assessment: Can Renewable Energy Replace Fossil Fuels by 2050?,” *Sustainability*, vol. 14, no. 8, p. 4792, 2022, doi: https://doi.org/10.3390/su14084792.

[9] T. H. Mamoona Riffat, Hassan Ali, H.A. Qayyum, M. Bilal, “Enhanced solar-driven water splitting by ZnO/CdTe heterostructure thin films-based photocatalysts,” *Int. J. Hydrogen Energy*, vol. 48, no. 58, pp. 22069–22078, 2023, [Online]. Available: https://www.sciencedirect.com/science/article/abs/pii/S0360319923010820?via%3Dihub

[10] M. I. Usman Qumar, Jahan Zeb Hassan, Rukhsar Ahmad Bhatti, Ali Raza, Ghazanfar Nazir, Walid Nabgan, “Photocatalysis vs adsorption by metal oxide nanoparticles,” *J. Mater. Sci. Technol.*, vol. 131, pp. 122–166, 2022, [Online]. Available: https://www.sciencedirect.com/science/article/abs/pii/S1005030222004728

[11] A. A. Mohd Raub *et al.*, “Photocatalytic activity enhancement of nanostructured metal-oxides photocatalyst: a review,” *Nanotechnology*, vol. 35, no. 24, Jun. 2024, doi: 10.1088/1361-6528/AD33E8,.

[12] J. Qi, W. Zhang, and R. Cao, “Solar-to-Hydrogen Energy Conversion Based on Water Splitting,” *Adv. Energy Mater.*, vol. 8, no. 5, p. 1701620, Feb. 2018, doi: 10.1002/AENM.201701620.

[13] Y. Zhao, Z. Niu, J. Zhao, L. Xue, X. Fu, and J. Long, "Recent Advancements in Photoelectrochemical Water Splitting for Hydrogen Production," *Electrochem. Energy Rev. 2023 61*, vol. 6, no. 1, pp. 1–46, Mar. 2023, doi: 10.1007/S41918-022-00153-7.

[14] P. Zhou *et al.*, "Solar-to-hydrogen efficiency of more than 9% in photocatalytic water splitting," *Nature*, vol. 613, no. 7942, pp. 66–70, Jan. 2023, doi: 10.1038/S41586-022-05399-1;SUBJMETA=4050,4077,4101,638,639,77,890,909;KWRD=ARTIFICIAL+PHOTOSYNTHESIS,PHOTOCATALYSIS.

[15] C. X. Wen-Hui Cheng, Alberto de la Calle Harry A. Atwater, Ellen B. Stechel, "Hydrogen from Sunlight and Water: A Side-by-Side Comparison between Photoelectrochemical and Solar Thermochemical WaterSplitting," *ACS Energy Lett.*, vol. 6, no. 9, 2021, [Online]. Available: https://pubs.acs.org/doi/10.1021/acsenergylett.1c00758

[16] Narendra M. Gupta, "Factors affecting the efficiency of a water splitting photocatalyst: A perspective," *Renew. Sustain. Energy Rev.*, vol. 71, pp. 585–601, 2017, [Online]. Available: https://www.sciencedirect.com/science/article/abs/pii/S1364032116311418?via%3Dihub

[17] Ç. Oruç, A. Çelik-Bozdoğan, G. Kurt-Gür, A. Aşıkoğlu-Bozkurt, and H. M. Luş, "Determination of the Optimum Annealing Temperature in the Production of CuO Nanoparticles with Antimicrobial Properties," *Nano*, vol. 17, no. 2, Feb. 2022, doi: 10.1142/S179329202250014X/ASSET/IMAGES/LARGE/S179329202250014X.JPEG.

[18] T. A. Shifa, F. Wang, Y. Liu, and J. He, "Heterostructures Based on 2D Materials: A Versatile Platform for Efficient Catalysis," *Adv. Mater.*, vol. 31, no. 45, p. 1804828, Nov. 2019, doi: 10.1002/ADMA.201804828;REQUESTEDJOURNAL:JOURNAL:15214095;WGROUP:STRING:PUBLICATION.

[19] Zhengyang CaiBilu Liu*Xiaolong ZouHui-Ming Cheng, "Chemical Vapor Deposition Growth and Applications of Two-Dimensional Materials and Their Heterostructures," *Chem. Rev.*, vol. 118, no. 13, 2018, [Online]. Available: https://pubs.acs.org/doi/10.1021/acs.chemrev.7b00536

[20] Ting KangTsz Wing TangBaojun PanHongwei LiuKenan ZhangZhengtang Luo, "Strategies for Controlled Growth of Transition Metal Dichalcogenides by Chemical Vapor Deposition for Integrated Electronics," *ACS Mater. Au*, vol. 2, no. 6, 2022, [Online]. Available: https://pubs.acs.org/doi/10.1021/acsmaterialsau.2c00029

[21] V A Gevorkyan et al, "Characterization of Cu2 O thin films prepared by evaporation of CuO powder," *J. Phys. Conf. Ser. Ser.*, vol. 350, p. 012027, 2012, [Online]. Available: https://iopscience.iop.org/article/10.1088/1742-6596/350/1/012027/pdf

[22] R. R. Pai, T. T. John, M. Lakshmi, K. P. Vijayakumar, and C. S. Kartha, "Observation of phase transitions in chemical bath deposited copper selenide thin films through conductivity studies," *Thin Solid Films*, vol. 473, no. 2, pp. 208–212, 2005, [Online]. Available: https://www.sciencedirect.com/science/article/abs/pii/S0040609004004663?via%3Dihub

[23] M. Z. Longbin Li, Yifang Zhao, Chaosheng Shi, Wei Zeng, Bing Liao, "Facile synthesis of copper selenides with different stoichiometric compositions and their thermoelectric performance at a low temperature range," *RSC Adv.*, vol. 42, 2021, [Online]. Available: https://pubs.rsc.org/en/content/articlelanding/2021/ra/d1ra04626h